The Canadian Mineralogist
Vol. 40, pp. 799-814 (2002)

Nb AND Ta OXIDE MINERALS IN THE FONTE DEL PRETE GRANITIC PEGMATITE DIKE, ISLAND OF ELBA, ITALY

CARLO AURISICCHIO§

Istituto di Geoscienze e Georisorse, Sezione di Roma, C.N.R., p.le A. Moro 5, I-00185 Roma, Italy

CATERINA DE VITO AND VINCENZO FERRINI

Dipartimento di Scienze della Terra, Università di Roma "La Sapienza", p.le A. Moro 5, I-00185 Roma, Italy

PAOLO ORLANDI

Dipartimento di Scienze della Terra, Università di Pisa, via S. Maria 53, I-56126 Pisa, Italy

ABSTRACT

The Fonte del Prete rare-element-enriched granitic pegmatite dike, located near the village of San Piero in Campo, Island of Elba, Italy, displays LCT-type geochemical features, and is genetically related to the Monte Capanne pluton. The dike is characterized by complex asymmetrical zoning, with miarolitic pockets containing primitive or highly evolved assemblages. There is a noteworthy presence of Nb and Ta oxides and complex oxides, occurring mainly in the pockets. Euxenite-(Y), polycrase-(Y), U–Bi-rich polycrase-(Y), and ferrocolumbite occur in the primitive pockets in the central part (core zone), whereas U–Bi-rich polycrase-(Y), uranopolycrase, manganocolumbite, manganotantalite, "wolframo-ixiolite", titanowodginite and microlite are found in the evolved pockets, at the extremities of the dike. Niobian rutile and euxenite-(Y) are also found in the massive pegmatite. The crystal chemistry and properties of the Nb and Ta oxides, as revealed by X-ray-diffraction studies, permit a reconstruction of the last stages of crystallization within each environment. During the evolution of the pegmatite, a volatile-rich melt with a high content of rare elements reached saturation in aqueous vapor. Minerals of Ti, Nb, Fe, Y + HREE occur in the primitive pockets; the enrichment of Mn, Ta and W in the evolved ones led to the crystallization of minerals with high Ta/(Ta + Nb) and Mn/(Mn + Fe) values, such as manganotantalite, microlite and titanowodginite. The polycrase-(Y) is unusually enriched in Bi and U, and is zoned from a Bi-poor core to a Bi-rich rim.

Keywords: complex granitic pegmatite, miarolitic pockets, Nb–Ta oxides, crystal chemistry, Monte Capanne pluton, Isola d'Elba, Italy.

SOMMAIRE

Le filon de pegmatite granitique à éléments rares de Fonte del Prete, situé près du village de San Piero in Campo, île d'Elbe, en Italie, fait preuve d'une tendance géochimique de type LCT et d'une affiliation avec le pluton de Monte Capanne. Le filon montre une zonation complexe assymétrique, avec des cavités miarolitiques contenant des assemblages plutôt primitifs ou fortement évolués. Les minéraux accessoires comprennent en particulier des oxydes de Nb et de Ta et des oxydes complexes, surtout dans les cavités. L'euxénite-(Y), la polycrase-(Y), une variété de polycrase-(Y) riche en Bi et U, et ferrocolumbite sont caractéristiques des cavités plutôt primitives de la partie centrale du filon, tandis que la polycrase-(Y) riche en Bi et U, l'uranopolycrase, la manganocolumbite, la manganotantalite, la "wolframo-ixiolite", la titanowodginite et la microlite sont typiques des cavités plutôt évoluées, vers les terminaisons du filon. Le rutile niobifère et l'euxénite-(Y) ont aussi été trouvés dans la pegmatite massive. La cristallochimie et les propriétés des oxydes de Nb et Ta en diffraction X permettent une reconstruction des derniers stades de la cristallisation dans chaque milieu. Au cours de l'évolution de la pegmatite, un magma enrichi en phase volatile avec une teneur élevée en éléments rares a atteint la saturation en phase aqueuse. Les minéraux de Ti, Nb, Fe, Y + terres rares lourdes se sont formés dans les cavités primitives; l'enrichissement en Mn, Ta et W dans les cavités évoluées a mené à la cristallisation de minéraux ayant des valeurs élevées de Ta/(Ta + Nb) et Mn/(Mn + Fe), comme la manganotantalite, la microlite et la titanowodginite. La polycrase-(Y) montre un enrichissement inhabituel en Bi et U; les cristaux sont zonés en Bi, d'un coeur pauvre à une bordure enrichie.

(Traduit par la Rédaction)

Mots-clés: pegmatite granitique complexe, poches miarolitiques, oxydes de Nb–Ta, cristallochimie, pluton de Monte Capanne, île d'Elbe, Italie.

§ *E-mail address*: aurisicchio@axrma.uniroma1.it

Introduction

Many investigators have dealt with models of pegmatite evolution based on the fractionation of the pairs Nb–Ta and Fe–Mn in Nb–Ta oxides and Ti–Nb–Ta complex oxides (Černý 1982, 1991, Černý & Ercit 1989, Mulja *et al.* 1996). In the granitic pegmatites of Elba, in Italy, the presence of numerous groups of oxides and complex oxides offers the opportunity to follow the spatial and temporal details of fractionation, involving not only the main elements Nb, Ta, Fe, and Mn, but also minor and trace elements like U, Bi, Y and the rare-earth elements (*REE*). Our paper focuses on the electron-microprobe-based chemical compositions and on XRD-based analyses of the degree of order of these oxide phases found in the Fonte del Prete dike, one of the bodies of granitic pegmatite found on the southeastern side of the Monte Capanne pluton, on the Island of Elba, near the village of San Piero in Campo. Bodies of granitic aplite and pegmatite in the area are well known to mineral collectors for the availability of gem-quality minerals, such as beryl and tourmaline. They show a complex and asymmetrical pattern of zoning (Pezzotta 2000).

Until relatively recently, investigators of the Elban pegmatites simply catalogued the mineralogical species found. In the last few years, however, research projects have been developed to reconstruct the texture and internal structure of these bodies, and to define the mineral assemblages of the bodies of granitic pegmatite, as well as their geochemical and petrochemical features (Pezzotta 1993, Aurisicchio *et al.* 1994, 1998a, b, De Vito 1998). In this contribution, we attempt to understand the evolution of the Fonte del Prete pegmatite on the basis of Nb- and Ta-bearing phases found in the primitive and evolved pockets.

Geological Setting

The Elban aplitic–pegmatitic dikes are closely linked to the history of the Monte Capanne pluton (Fig. 1). Two systems of fractures are present: the main one is radial, whereas the second set has a NNE–SSW trend. In the San Piero in Campo and Sant'Ilario area, the latter fractures are filled by aplitic–pegmatitic material (Boccaletti & Papini 1989). In many cases, such dikes cross the margin of the pluton into the surrounding contact-metamorphic aureole (Keller & Pialli 1990). The Monte Capanne pluton and the pegmatite dikes were emplaced 6.7–6.9 Ma ago, as determined by a Rb–Sr whole-rock isochron (Ferrara & Tonarini 1985).

These bodies are exposed in outcrops or in quarries (20 m maximum along strike) and are aligned in such a way as to suggest that they are segments of a single dike or a series of parallel veins. The predominant rock-type in the pluton is a mildly peraluminous monzogranite with an inequigranular texture; this monzogranite contains large megacrysts of K-feldspar, which are abundant in the border zones of the pluton, in leucogranites and in "evolved facies" (Poli *et al.* 1989). These evolved facies are represented by microgranites, bodies of aplite, and pegmatite with lower biotite:tourmaline ratio and, in some cases, with a total absence of biotite (Poli *et al.* 1989). According to these authors, the various facies of the pluton are ascribed to a complex process of mixing involving a peraluminous magma formed by partial melting of metasedimentary rocks and batches of mantle-derived basic magma of potassic affinity, followed by fractional crystallization (Poli *et al.* 1989).

The crystal-chemistry study reported here was carried out on samples of the Fonte del Prete dike. It belongs to the pegmatitic field cropping out in the San Piero in Campo area, which includes famous quarries like La Speranza, Masso Forese, Fonte del Prete, Facciatoia, Grotta d'Oggi, and Fosso Gorgolinato. These dikes display a variable strike, inclination, thickness, and mineralogical composition, and have informally been classified as Li-bearing dikes with complex asymmetrical zoning (Pezzotta 2000, Orlandi & Pezzotta 1997) (Fig.1).

A distinctive characteristic of these bodies is the presence of small pockets (~1 cm in size), mainly in the central part and at the terminations of the dike, along its strike. Those pockets located in the core zone contain schorl, blue beryl, spessartine, ilmenorutile, ferrocolumbite, euxenite-(Y), polycrase-(Y) and U–Bi-rich polycrase-(Y). Those pockets that are irregularly distributed at the terminations of the dike, are characterized by polychrome tourmaline, colorless beryl, Li-dominant minerals (mainly lepidolite), manganocolumbite, U-Bi-rich polycrase-(Y), uranopolycrase, microlite, an unidentified W-rich phase, wodginite and, rarely, manganotantalite.

At the present time, the Fonte del Prete dike cannot be mapped because coarse debris covers the exposure in the quarry. However, a reconstruction of its complex asymmetrical zoning (Fig. 2) was produced with the aid of information from former employees at the quarry and on the basis of the close similarity to other dikes cropping out in the area. The samples analyzed in this paper have been supplied by local workers. The geological features described by them about texture, fabric and location of the miarolitic pockets are consistent with the features revealed in the large dumps in the area.

Experimental Methods

The samples studied were selected from the two type of pockets mentioned above; a few others come from the massive pegmatite in its intermediate zone, in the central part of the dike. The small size (a few mm) and striking compositional zoning shown by Nb and Ta oxides in the Fonte del Prete suite required electron-microprobe (EMP) data and, where possible, X-ray-diffraction (XRD) analysis to determine their composition

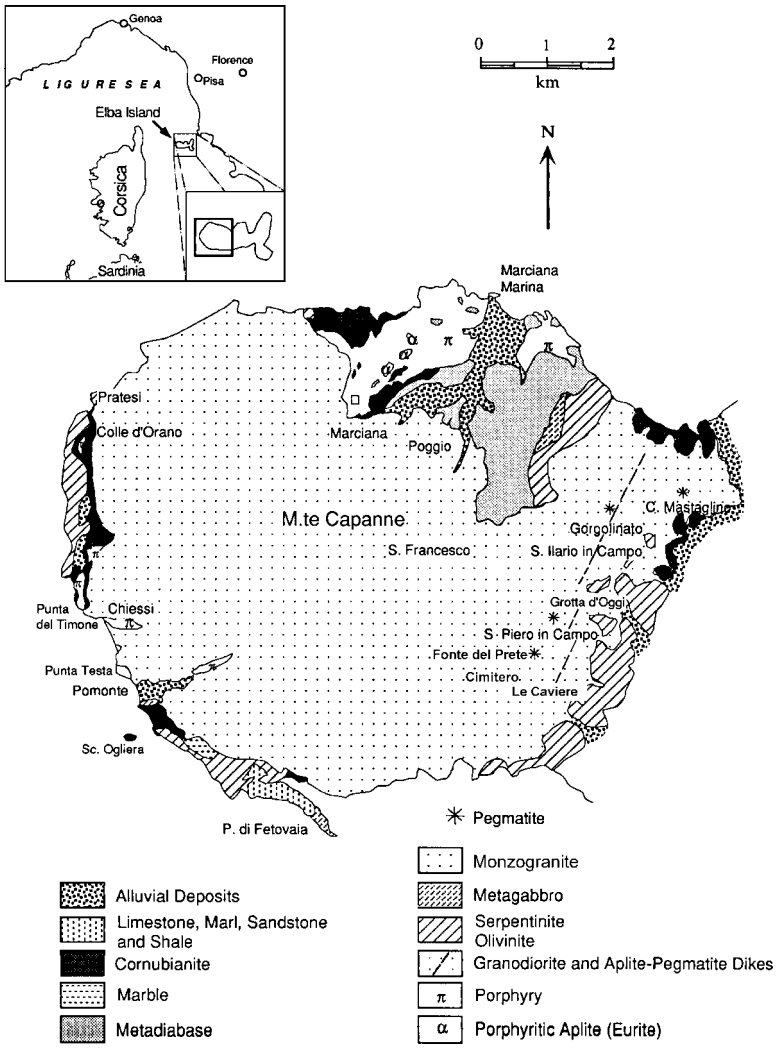

FIG. 1. Geological map of the eastern margin of the Monte Capanne pluton, island of d'Elba, Italy, where the Fonte del Prete dike of granitic pegmatite is exposed.

and unit-cell parameters. The EMP analyses of the Nb and Ta oxides were done with a Cameca Cx 827 instrument equipped with three wavelength-dispersion spectrometers (WDS) and one energy-dispersion spectrometer (EDS, Link Systems AN 10000/85S), at the IGG–CNR, the University of Rome "La Sapienza". All samples were analyzed with an accelerating voltage of 15 kV, a sample current of 30 nA measured on synthetic andradite, and a beam diameter of 3 μm. Wavelength-dispersion spectrometers were used for the following elements: *K*α lines for F, Na, Mg, Al, Si, Ca, Fe, Mn, Ti, and Sc, *L*α for Y, Zr, Nb, Sn and W, and *M*α for Ta, Pb, Bi, Th and U. Element peaks and backgrounds (WDS) were measured with counting times of 10 s each. A glass of diopside composition was used as a reference standard for Si, Ca and Mg, fluorapatite for F, jadeite for Al and Na, rutile for Ti, fayalite for Fe, rhodonite for Mn, synthetic Sc_2O_3 oxide for Sc, ZrO_2 for Zr, $LiNbO_3$ for Nb, cassiterite for Sn, $CaWO_4$ for W, $LiTaO_3$ for Ta, galena for Pb, Bi metal, thorite for Th, and UO_2 for U.

The electron-microprobe analysis of minerals containing the *REE* was complicated because of the overlap of peaks of the *L* series; *L*α was used for Ce, Pr, Nd,

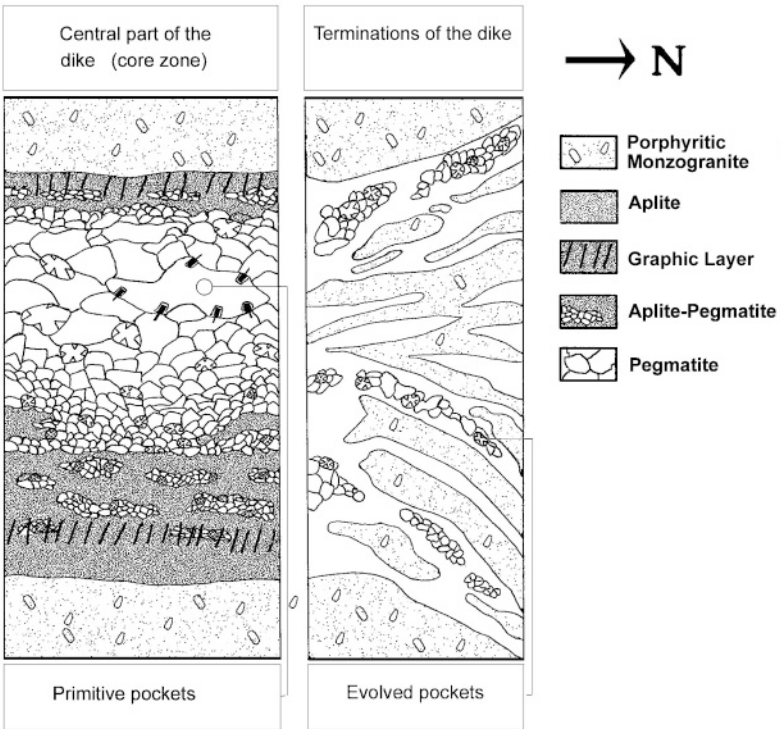

FIG. 2. N–S cross-section of the Fonte del Prete dike. Left panel: central part with its asymmetrical zoning and primitive pockets (core zone). Right panel: extremities of the dike, with irregularly distributed veins, showing coarse grain-size and evolved pockets.

Gd, Er and Yb, and Lβ was used for Sm, Ho and Dy. The others REE were not included in the processing, since they were below detection limits. Peaks and backgrounds for each *REE* were measured according to the approach of Roeder (1985). Synthetic silicate glasses (Drake & Weill 1972, Åmli & Griffin 1975) were used for quantitative determination of *REE* concentrations. Corrections for the matrix effect were calculated by ZAF software (Microbeam Service). The analytical error was ~1% relative for major elements, and ~5% relative for minor elements. Detection limits at the working conditions specified ranged between 0.05 and 0.1 wt.%.

X-ray-diffraction analyses were carried out at the Department of Earth Sciences of the University of Pisa, using a Gandolfi camera (114.6 mm diameter, Fe*K*α radiation). Unit-cell parameters were calculated, after correction for shrinkage, by least-squares refinement of powder-diffraction patterns using the program of Appleman & Evans (1973), as modified by Garvey (1986). Because of sample size, chemical heterogeneity and metamict state, it was not always possible to obtain a pattern that could be indexed for these samples.

CRYSTAL CHEMISTRY

Niobian rutile

The Nb-enriched, Fe-bearing variety of rutile, with general formula $(Ti,Nb,Fe,Ta,Sn)O_2$ forms black, vitreous subhedral crystals 2 mm across, in the intermediate zone of the pegmatite and rarely in the primitive pockets of the core zone. The unit-cell parameters and composition are reported in Table 1. Analyzed grains are very homogeneous and do not show any evidence of an intergrowth of other phases.

Following the suggestion of Černý *et al.* (1981), the formula was calculated on the basis of four anions and two cations (Table 1). Ti is the dominant element, attaining 1.5 atoms per formula unit (*apfu*). The remaining 0.5 *apfu* consists of Nb (0.20–0.22 *apfu*), Fe^{3+} (0.18–0.20 *apfu*), Sn (0.04–0.05 *apfu*), and Ta (0.02–0.04 *apfu*). These elements seem controlled by the substitution scheme: $Fe^{3+} + (Nb,Ta)^{5+} \Leftrightarrow Ti^{4+} + Sn^{4+}$. The correlation $Fe^{3+} + (Nb,Ta)^{5+}$ *versus* $Ti^{4+} + Sn^{4+}$ shows a striking negative trend, as expected by the suggested mechanism of substitution.

Euxenite group

Complex metamict Ti–Nb–Ta oxides with the general formula AB_2O_6 occur as members of the euxenite–polycrase group (Ewing 1976, Ewing *et al.* 1977), with a prismatic habit elongate in the *c* direction. Euxenite-(Y), the Nb-dominant phase stable at high temperature (Ewing & Ehlmann 1975, Ewing 1976, Aurisicchio *et al.* 2001), occurs in the intermediate zone of the pegmatite, associated with cassiterite and niobian rutile, and rarely in the primitive pockets of the core zone. Polycrase-(Y) occurs in the primitive pockets, together with columbite, tourmaline, and beryl. Its composition shows high Ti contents at the *B* site, whereas the *A* site (Y, U, Bi, Th, *REE*, Ca, Mn) shows a wide chemical variability. The samples from the Fonte del Prete dike show trends from Y-rich to U-rich compositions. The trend is evident among crystals or in zoned grains. Table 2 lists the compositions of some of the samples studied; these were selected so as to emphasize the trends observed.

For the first time, we report polycrase compositions enriched in Bi. The Bi analytical value cannot be considered overestimated, as these samples show a very low amount of Ce, whose $L\alpha$ line does overlap with Bi$M\alpha$.

TABLE 1. REPRESENTATIVE COMPOSITIONS OF NIOBIAN RUTILE, FONTE DEL PRETE DIKE, ISLAND OF ELBA, ITALY

Sample	i.z. IR1	i.z. IR2	i.z. IR3	p. p. IR4	p. p. IR5	p. p. IR6	p. p. IR7	p. p. IR8
CaO wt%	0.43	0.00	0.14	0.00	0.07	0.08	0.03	0.06
MgO	0.00	0.03	0.13	0.08	0.00	0.02	0.14	0.02
MnO	0.00	0.00	0.00	0.00	0.00	0.00	0.00	0.03
FeO	1.66	1.92	1.60	2.10	2.25	2.20	1.66	1.94
Al_2O_3	0.48	0.49	0.55	0.59	0.35	0.56	0.51	0.48
Fe_2O_3	6.68	6.06	7.29	6.35	6.32	6.19	6.96	6.75
Nb_2O_5	15.60	15.65	16.71	16.39	16.41	16.48	16.69	16.13
Ta_2O_5	4.86	2.52	3.50	4.01	3.53	3.93	2.88	3.59
TiO_2	66.34	67.81	64.91	64.97	65.16	64.60	65.45	64.50
SnO_2	0.00	4.08	3.79	3.89	3.34	3.41	3.80	3.69
WO_3	1.78	1.32	1.92	1.41	1.36	1.36	1.47	1.65
Total	97.83	99.88	100.54	99.79	98.79	98.83	99.59	98.84
Structural formulae based on four anions and two cations								
Ca *apfu*	0.014	0.000	0.004	0.000	0.002	0.003	0.001	0.002
Mg	0.000	0.001	0.006	0.004	0.000	0.001	0.006	0.001
Mn^{2+}	0.000	0.000	0.000	0.000	0.000	0.000	0.000	0.001
Fe^{2+}	0.042	0.048	0.040	0.053	0.057	0.056	0.041	0.049
Al	0.017	0.017	0.019	0.021	0.012	0.020	0.018	0.017
Fe^{3+}	0.152	0.135	0.163	0.143	0.144	0.141	0.156	0.154
Nb	0.213	0.210	0.225	0.222	0.224	0.225	0.226	0.221
Ta	0.040	0.020	0.028	0.033	0.029	0.032	0.023	0.030
Ti	1.508	1.511	1.454	1.467	1.481	1.470	1.471	1.469
Sn	0.000	0.048	0.045	0.047	0.040	0.041	0.045	0.045
W^{6+}	0.014	0.010	0.015	0.011	0.011	0.011	0.011	0.012
Σ cations	2.000	2.000	1.999	2.001	2.000	2.000	1.998	2.001

i.z.: intermediate zone of the massive pegmatite; p.p.: primitive pockets. The ratio of Fe^{2+} to Fe^{3+} is calculated on the basis of charge balance in a formula of four oxygen atoms and 2 cations. Unit-cell parameters of sample IR7: *a* 4.621(3), *c* 2.981(2) Å. In this and following tables, cation proportions are quoted in atoms per formula unit (*apfu*).

Bismuth occupies the *A* site of polycrase and shows a negative correlation with Y. The few compositions of euxenite obtained indicate a lack of Bi.

The first sample mentioned in Table 2 (H14) shows a core with Nb > Ti, whereas the rim of the grain is Ti-dominant. Figure 3 shows X-ray maps of sample H14 for Nb (a), Ti (b), Y (c), and Bi (d). Of course, the color scale used for the X-ray maps cannot reveal small variations in element content (Table 2); whereas Nb and Y show sharp chemical variations that are well described in the photos, Ti and Bi (mainly Ti) show moderate variations, and would seem to have a crudely homogeneous distribution. The compositional data agree with a transition from an euxenite-dominant core to a polycrase rim. Niobium and Y increase together, with a maximum of concentration in the euxenite core; the proportion of Bi and Ti is greater near the crystal rim, forming the polycrase area.

Sample X3, with Ti > Ta > Nb in the *B* site, and Y > U in the *A* site, can be considered a more evolved composition of polycrase-(Y), on the basis of the Ta/(Ta + Nb) value (0.53). Sample 1152 shows an intergrowth of ferrocolumbite + polycrase-(Y). Sample 2155 provides a new example of uranopolycrase, with U contents in a few cases greater than those published in Aurisicchio *et al.* (1993). The remaining compositions are all examples of polycrase-(Y), with compositions that vary according to whether they have been found in the primitive or evolved pockets of the Fonte del Prete dike. The dominant *B*-site cation is Ti, approximately 1.1 *apfu* (Table 2), whereas the content of Nb and Ta shows much variability. Figure 4 shows the distribution of the euxenite-group minerals found in the primitive and evolved pockets, on the basis of the *B*-site occupancy. Whereas the primitive pockets contain euxenite-(Y) and polycrase-(Y), only in the evolved pockets was the Ti-dominant phase found. Figure 5 shows the occupancy of the *A* site for material from the primitive and evolved pockets. The general trend shows the increase in U and the decrease in Y (+ *REE*) in the more evolved cavities. In some cases, Bi follows the increase in uranium, reaching a maximum of 0.2 *apfu* (Table 2).

The compositional variation of these phases reflects the composition of the pegmatite-forming melt – fluid system in the two pocket environments. The exsolved aqueous fluid, in the core zone, is less evolved than that at the terminations of the dike. Therefore, the latter pockets represent the last stage of crystallization within the host pegmatite.

Samples H14, X3, and 2155 were analyzed by XRD to determine their unit-cell parameters after heating at 900°C for ten hours. Table 2 lists the results calculated on the basis of the space group *Pbcn*. The sample of polycrase-(Y) number 2155 shows a shorter *a* parameter than the other two samples (Table 2). This behavior confirms the distortion of the coordination polyhedron around the U cations in the *A* site, as suggested by Aurisicchio *et al.* (1993). The *A* polyhedron may be

TABLE 2. REPRESENTATIVE COMPOSITIONS OF MEMBERS OF THE EUXENITE GROUP OF MINERALS, FONTE DEL PRETE DIKE, ISLAND OF ELBA, ITALY

Sample	p. p. H14 core	p. p. H14 rim	p. p. X3 rim	p. p. 1152 core	p. p. 1152 rim	p. p. 2929 core	p. p. 2929 rim	p. p. 2931 mean*	e. p. 1185 core	e. p. 1185 interior	e. p. 1185 rim	e. p. 2154 mean¶	e. p. 2155 core	e. p. 2155 rim
Na_2O wt%	0.32	0.35	0.69	0.00	0.00	0.00	0.00	0.00	0.00	0.00	0.00	0.00	0.00	0.00
MgO	0.51	0.49	0.39	0.34	0.33	0.85	0.47	0.56	0.00	0.00	0.00	0.00	0.25	0.44
CaO	1.10	1.19	1.05	0.68	0.89	0.91	0.87	0.71	0.99	0.74	1.03	0.54	0.38	0.35
FeO	0.30	1.68	0.22	0.00	0.71	0.32	0.80	0.31	0.82	1.13	1.53	0.56	0.68	0.00
MnO	1.15	0.38	1.42	0.94	0.68	0.00	0.00	0.00	1.46	0.00	0.75	0.13	1.66	1.18
UO_2	8.26	10.45	12.51	13.01	12.82	8.70	11.39	8.76	13.12	11.83	13.34	19.45	36.55	35.51
ThO_2	0.81	1.75	2.48	1.74	2.32	2.83	3.65	4.07	1.60	2.44	2.22	1.79	2.36	2.50
PbO	0.33	0.71	0.46	0.99	0.00	2.02	1.03	2.44	0.00	2.61	1.42	0.40	0.32	0.00
Bi_2O_3	0.00	9.37	1.59	0.00	6.65	9.46	11.56	0.00	0.36	11.32	12.85	0.36	0.00	0.20
Y_2O_3	15.83	9.08	12.48	13.79	10.34	10.46	7.53	12.66	13.92	8.61	7.30	13.94	6.37	8.08
Ce_2O_3	0.00	0.00	0.00	0.00	0.00	1.32	1.15	0.00	0.00	0.00	0.00	0.00	0.00	0.00
Nd_2O_3	0.40	0.62	0.00	0.00	0.00	0.00	0.00	0.00	0.00	0.00	0.00	0.00	0.00	0.00
Sm_2O_3	0.00	0.00	0.00	0.00	0.00	0.00	0.00	0.00	0.65	0.47	0.74	0.84	0.00	0.00
Dy_2O_3	0.00	0.00	0.00	2.87	1.02	2.27	1.75	2.80	1.81	1.58	1.47	1.46	1.15	1.85
Er_2O_3	0.00	0.00	0.00	0.00	0.00	1.49	0.52	0.00	0.00	0.00	0.00	0.00	0.00	0.00
Yb_2O_3	0.00	0.00	0.00	3.65	1.72	0.00	0.00	3.23	2.22	0.00	0.00	0.00	1.33	0.81
Nb_2O_5	34.62	22.47	14.58	21.78	18.26	24.31	18.85	26.41	28.67	18.60	16.34	23.16	11.19	16.48
Ta_2O_5	14.79	17.58	27.04	16.43	19.25	7.14	8.77	7.10	11.62	16.73	16.53	9.61	9.87	5.73
TiO_2	18.04	19.67	18.13	20.87	20.63	22.85	23.88	24.99	18.92	18.45	17.64	24.16	24.49	25.47
WO_3	0.69	1.48	6.26	2.19	4.31	4.45	4.19	4.47	2.08	4.80	6.21	2.24	0.97	0.87
Al_2O_3	0.42	0.33	0.00	0.52	0.75	0.89	0.73	0.69	0.55	0.70	0.77	0.44	0.38	0.27
Total	97.57	97.60	99.30	99.80	100.68	100.27	97.14	99.20	98.79	100.01	100.15	99.08	97.94	99.74
Structural formulae based on six atoms of oxygen														
Na *apfu*	0.038	0.045	0.092	0.000	0.000	0.000	0.000	0.000	0.000	0.000	0.000	0.000	0.000	0.000
Mg	0.047	0.049	0.040	0.033	0.033	0.080	0.047	0.051	0.000	0.000	0.000	0.000	0.027	0.040
Ca	0.072	0.085	0.076	0.047	0.063	0.062	0.063	0.047	0.068	0.055	0.078	0.037	0.029	0.025
Fe	0.015	0.094	0.012	0.000	0.039	0.017	0.045	0.016	0.043	0.066	0.090	0.030	0.041	0.000
Mn	0.060	0.022	0.082	0.052	0.038	0.000	0.000	0.000	0.079	0.000	0.045	0.007	0.100	0.070
U	0.112	0.156	0.189	0.187	0.188	0.123	0.170	0.119	0.186	0.183	0.210	0.274	0.581	0.534
Th	0.011	0.027	0.038	0.026	0.035	0.041	0.056	0.057	0.023	0.039	0.036	0.026	0.038	0.040
Pb	0.005	0.013	0.008	0.017	0.000	0.035	0.019	0.040	0.000	0.049	0.027	0.007	0.006	0.000
Bi	0.000	0.162	0.028	0.000	0.113	0.155	0.200	0.000	0.006	0.203	0.235	0.006	0.000	0.003
Y	0.515	0.324	0.452	0.475	0.363	0.353	0.269	0.412	0.471	0.319	0.276	0.470	0.242	0.291
Ce	0.000	0.000	0.000	0.000	0.000	0.031	0.028	0.000	0.000	0.000	0.000	0.000	0.000	0.000
Nd	0.009	0.015	0.000	0.000	0.000	0.000	0.000	0.000	0.000	0.000	0.000	0.000	0.000	0.000
Sm	0.000	0.000	0.000	0.000	0.000	0.000	0.000	0.000	0.014	0.011	0.018	0.018	0.000	0.000
Dy	0.000	0.000	0.000	0.060	0.022	0.046	0.038	0.055	0.037	0.035	0.034	0.030	0.026	0.040
Er	0.000	0.000	0.000	0.000	0.000	0.032	0.012	0.000	0.000	0.000	0.000	0.000	0.000	0.000
Yb	0.000	0.000	0.000	0.072	0.035	0.000	0.000	0.060	0.000	0.000	0.000	0.000	0.029	0.017
A site	0.885	0.991	1.018	0.969	0.928	0.975	0.947	0.856	0.927	0.960	1.049	0.904	1.119	1.061
Nb	0.958	0.680	0.449	0.637	0.545	0.698	0.573	0.730	0.824	0.585	0.523	0.663	0.361	0.504
Ta	0.246	0.320	0.501	0.289	0.346	0.123	0.160	0.118	0.201	0.317	0.319	0.166	0.192	0.105
Ti	0.830	0.991	0.928	1.015	1.024	1.091	1.207	1.149	0.902	0.966	0.940	1.151	1.315	1.295
W	0.011	0.026	0.110	0.037	0.074	0.073	0.073	0.071	0.034	0.087	0.114	0.037	0.018	0.015
Al	0.030	0.026	0.000	0.040	0.058	0.067	0.058	0.050	0.042	0.058	0.064	0.033	0.032	0.022
B site	2.075	2.043	1.987	2.018	2.046	2.051	2.071	2.117	2.003	2.013	1.960	2.050	1.918	1.941
Σcations	2.960	3.034	3.005	2.986	2.975	3.026	3.018	2.974	2.930	2.973	3.009	2.954	3.037	3.002

p.p.: primitive pockets, e.p.: evolved pockets. * mean result of eight determinations; ¶ mean result of sixteen determinations. Unit-cell parameters of selected samples: H14: *a* 14.630(1), *b* 5.632(2), *c* 5.188(1) Å; X3: *a* 14.640(3), *b* 5.571(3), *c* 5.237(5) Å; 2155: *a* 14.530(7), *b* 5.618(7), *c* 5.180(1) Å.

described as a distorted cube as well as a square antiprism; indeed, the two longest *A*–O distances are markedly different than the other six.

Columbite–tantalite group

Minerals of the columbite–tantalite group have the general formula AB_2O_6, with the *A* site occupied by Fe, Mn, and a smaller quantity of Mg, Na, and trivalent ions,

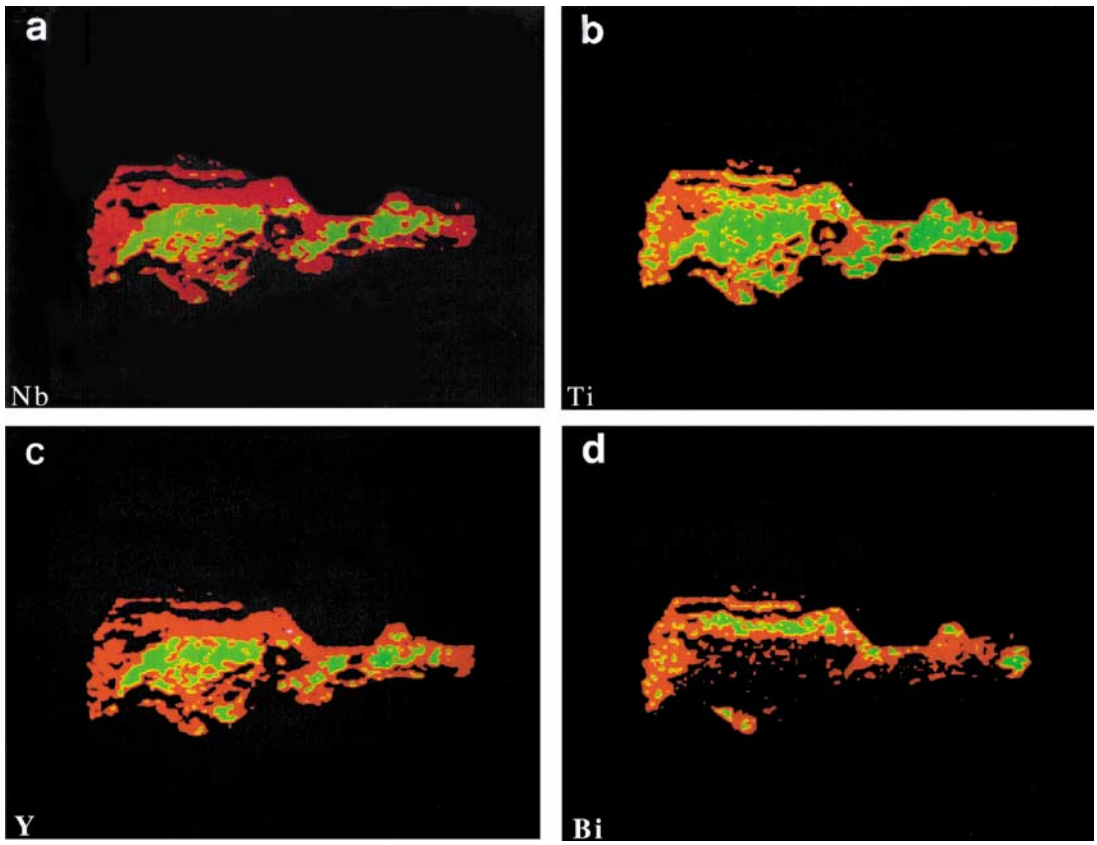

FIG. 3. X-ray maps of Nb (a), Ti (b), Y (c), and Bi (d) in sample H14, showing the trend from a core of euxenite-(Y) to a rim of polycrase-(Y). Magnification 80× (green > red).

and the *B* site occupied by Nb, Ta and small amounts of Ti and W. The main trends known from the literature are the isovalent substitutions Fe ↔ Mn in the *A* site, and Nb ↔ Ta in the *B* site, with corresponding end-members ferrocolumbite, manganocolumbite, ferrotantalite and manganotantalite (Ercit 1994, Ercit *et al.* 1995).

Table 3 shows the composition of some representative samples of columbite–tantalite from the Fonte del Prete dike. More than 200 analyses have been made of representative samples. Heterovalent substitutions involve the *A* site or the *B* site (or both). Na, Mg, Sn, Y, and the *REE* display extensive heterovalent isomorphism at the *A* site, whereas the coupled substitution of Ti + W for Nb + Ta occurs at the *B* site, as reported also by Mulja *et al.* (1996).

The columbite-group mineral from primitive pockets (core zone) is iron-dominant, and is widespread in the matrix and primary accessory phases such as tourmaline, blue beryl, cassiterite, euxenite-(Y)–polycrase-(Y), and garnet. In contrast, manganese-dominant varieties, evolving from manganocolumbite to manganotantalite, have been found in the evolved pockets (terminations of the dike), together with manganoan elbaite, pink to colorless beryl, lithium-rich phases, and an unknown W-rich phase, wodginite, and microlite.

The compositions reported in Table 3 show cation totals ranging from 2.986 to 3.060 *apfu*, suggesting the presence of trivalent cations. The Fonte del Prete samples show a variable WO_3 content ranging from 0 to 10 wt%. The TiO_2 content ranges from 1.5 to <7.0 wt% (Table 3). The presence of W and Ti in the structure of the columbite–tantalite phases confirms the heterovalent substitution for Nb and Ta according to the following mechanism: $2(Nb,Ta)^{5+} \leftrightarrow Ti^{4+} + W^{6+}$.

An increase in the content of the couple Ti–W promotes structural disorder, as shown by the unit-cell parameters of two heated crystals (Table 3): ferrocolumbite 2159 shows partial order (about 75% order: Ercit *et al.* 1995), likely because of its chemical hetero-

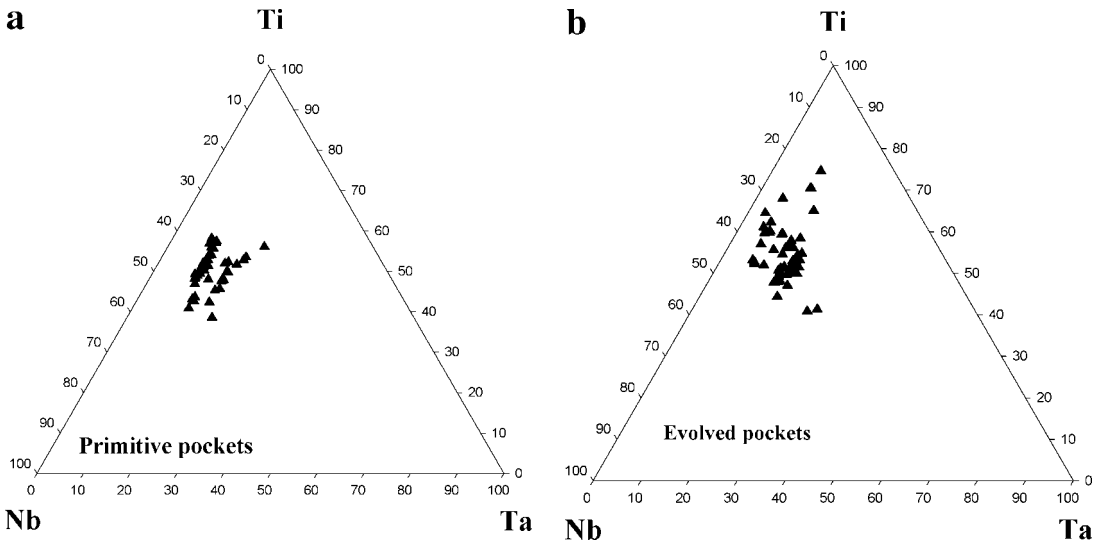

FIG. 4. Triangular plot of the *B*-site cations Ti–Nb–Ta in the euxenite group of minerals. (a) Primitive pockets, and (b) evolved pockets.

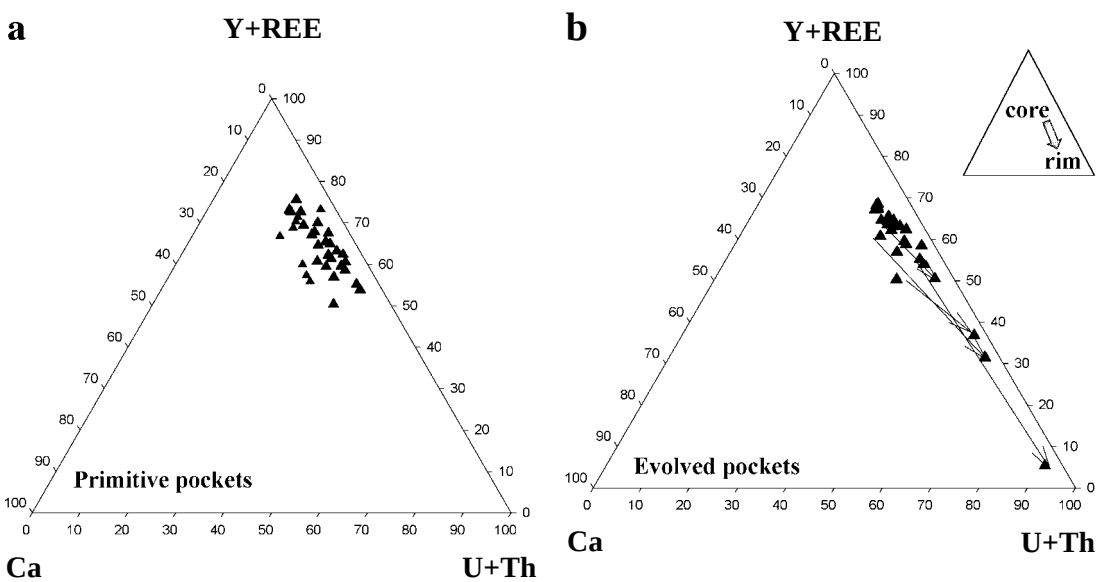

FIG. 5. Triangular plot of the *A*-site cations Y + *REE* – Ca – U + Th in the euxenite group of minerals. (a) Primitive pockets, and (b) evolved pockets.

geneity, and manganocolumbite 1144 has a value of the order parameter close to 100%.

In Figure 6, the occupancy of the *A* and *B* sites is considered. This diagram shows the striking compositional variation of the columbite–tantalite group. The Fonte del Prete dike, indeed, shows a high activity of W, as suggested by the constant presence of this element in the columbite–tantalite minerals. Figure 6 displays three compositional fields having an average W content near 2–3% (columbite–tantalite), 12% (manga-

TABLE 3. REPRESENTATIVE COMPOSITIONS OF COLUMBITE–TANTALITE FROM THE FONTE DEL PRETE DIKE, ISLAND OF ELBA, ITALY

Sample	p. p. 1188 core	p. p. 1188 rim	p. p. 2159 core	p. p. 2159 rim	p. p. 1152 a	p. p. 1152 b	e. p. 1158[I] core	e. p. 1158[II] rim	e. p. 1160 core	e. p. 1160 rim	e. p. 1144 core	e. p. 1144 rim	e. p. 1146 mean*	e. p. 1147 mean¶	e. p. 1149 mean§	e. p. 2157 core	e. p. 2157 core	e. p. 2157 rim	e. p. 2157 rim
Na_2O wt %	0.28	0.24	0.00	0.00	0.35	0.17	0.00	0.00	0.00	0.00	0.00	0.00	0.05	0.08	0.17	0.17	0.17	0.00	0.00
MgO	0.54	0.78	0.24	0.18	0.61	0.42	0.00	0.00	0.00	0.00	0.00	0.16	0.00	0.00	0.00	0.00	0.19	0.12	0.12
CaO	0.00	0.20	0.11	0.00	0.16	0.27	0.00	0.00	0.27	0.00	0.00	0.00	0.00	0.04	0.24	0.16	0.11	0.00	0.00
FeO	11.82	10.93	12.48	11.99	11.15	11.08	3.43	2.81	2.63	3.29	0.00	0.00	0.49	0.00	0.40	0.22	0.17	0.00	0.44
MnO	4.31	4.47	5.20	5.94	4.76	4.97	13.00	14.58	11.55	13.53	17.23	18.35	15.26	16.98	16.27	16.59	16.62	15.63	14.80
UO_2	0.00	0.00	0.35	0.00	0.00	0.00	0.00	1.07	2.71	0.00	0.00	0.00	0.58	0.35	1.29	0.00	0.00	0.00	0.00
SnO_2	0.55	0.00	0.00	0.00	0.00	0.30	0.00	0.00	0.00	0.00	0.47	0.00	0.44	0.23	0.86	0.56	0.38	0.72	0.98
Y_2O_3	0.00	0.00	0.38	0.83	0.00	0.00	0.00	0.00	2.45	1.61	0.00	0.00	1.09	0.82	0.00	0.46	0.00	0.00	0.00
Dy_2O_3	0.00	0.00	0.99	1.23	0.00	0.00	1.92	0.00	0.86	1.24	0.00	0.00	0.00	0.00	0.00	0.00	0.00	0.00	0.00
Yb_2O_3	0.00	1.97	0.00	0.00	0.00	0.00	1.49	1.75	1.10	0.00	1.46	0.00	0.00	0.00	0.00	0.00	0.00	0.00	0.00
Nb_2O_5	33.26	38.98	39.80	40.54	45.83	48.00	35.20	43.29	36.93	42.66	41.58	43.21	44.68	44.79	36.74	42.90	42.27	24.48	23.27
Ta_2O_5	32.49	34.54	26.50	26.88	29.49	25.78	30.02	26.03	27.23	27.38	27.03	27.20	32.55	33.49	37.68	36.26	35.68	57.81	58.69
TiO_2	4.86	4.16	4.22	4.04	4.12	3.19	3.82	3.35	5.06	3.45	2.62	3.01	3.78	2.51	4.72	0.93	1.11	0.88	0.76
WO_3	10.33	3.16	9.12	0.43	4.38	4.55	10.06	6.64	7.54	6.29	8.10	7.90	0.41	0.55	0.62	1.47	2.34	0.00	0.00
Al_2O_3	0.32	0.30	0.34	0.00	0.14	0.00	0.26	0.00	0.15	0.00	0.00	0.00	0.00	0.00	0.24	0.00	0.00	0.00	0.00
Total	98.75	99.73	99.72	100.65	100.98	98.73	99.19	99.50	99.49	99.44	99.23	99.83	99.34	99.85	99.23	99.73	99.03	99.63	99.43
Structural formulae based on six atoms of oxygen																			
Na *apfu*	0.036	0.030	0.000	0.000	0.042	0.021	0.000	0.000	0.000	0.000	0.000	0.000	0.010	0.020	0.020	0.022	0.022	0.000	0.000
Mg	0.054	0.076	0.023	0.017	0.056	0.040	0.000	0.000	0.000	0.000	0.000	0.016	0.000	0.000	0.000	0.000	0.019	0.013	0.013
Ca	0.000	0.014	0.008	0.000	0.011	0.018	0.000	0.000	0.011	0.000	0.000	0.000	0.000	0.010	0.020	0.012	0.008	0.000	0.000
Fe	0.654	0.594	0.671	0.639	0.579	0.586	0.192	0.152	0.147	0.177	0.000	0.000	0.030	0.000	0.030	0.012	0.009	0.000	0.027
Mn	0.242	0.246	0.283	0.321	0.250	0.266	0.736	0.798	0.752	0.739	0.955	0.994	0.830	0.930	0.900	0.926	0.932	0.966	0.924
U	0.000	0.000	0.000	0.000	0.000	0.000	0.000	0.015	0.013	0.000	0.000	0.000	0.050	0.010	0.020	0.000	0.000	0.000	0.000
Sn	0.014	0.000	0.000	0.000	0.000	0.007	0.000	0.000	0.000	0.000	0.012	0.000	0.010	0.010	0.015	0.015	0.010	0.021	0.029
Y	0.000	0.000	0.013	0.028	0.000	0.000	0.000	0.000	0.052	0.055	0.000	0.000	0.035	0.030	0.000	0.016	0.000	0.000	0.000
Ce	0.000	0.000	0.000	0.000	0.000	0.000	0.000	0.000	0.000	0.000	0.008	0.000	0.000	0.000	0.000	0.000	0.000	0.000	0.000
Dy	0.000	0.000	0.020	0.025	0.000	0.000	0.041	0.000	0.016	0.026	0.000	0.000	0.000	0.000	0.000	0.000	0.000	0.000	0.000
Yb	0.000	0.039	0.039	0.039	0.000	0.000	0.030	0.035	0.000	0.000	0.029	0.000	0.000	0.000	0.000	0.000	0.000	0.000	0.000
A site	1.000	1.000	1.023	1.030	0.944	0.938	1.000	1.000	0.990	0.998	1.014	1.010	0.965	1.010	1.005	1.002	1.000	0.999	1.003
Nb	0.995	1.147	1.157	1.168	1.287	1.372	1.064	1.266	1.162	1.244	1.231	1.250	1.280	1.290	1.088	1.278	1.266	0.807	0.775
Ta	0.585	0.611	0.464	0.466	0.498	0.443	0.546	0.458	0.502	0.480	0.481	0.473	0.560	0.580	0.670	0.650	0.643	1.147	1.176
Ti	0.242	0.204	0.204	0.193	0.192	0.152	0.192	0.163	0.181	0.167	0.129	0.145	0.180	0.120	0.230	0.046	0.055	0.048	0.042
W	0.177	0.053	0.152	0.142	0.070	0.075	0.174	0.111	0.136	0.105	0.137	0.131	0.010	0.020	0.025	0.025	0.040	0.000	0.000
Al	0.025	0.023	0.025	0.032	0.010	0.000	0.020	0.000	0.021	0.000	0.000	0.000	0.000	0.000	0.010	0.000	0.000	0.000	0.000
B site	2.024	2.038	2.003	2.001	2.058	2.041	1.997	1.997	2.003	1.997	1.978	1.999	2.030	2.010	2.023	1.999	2.003	2.002	1.994
Σcations	3.024	3.038	3.026	3.030	3.002	2.980	2.997	2.997	2.993	2.995	2.992	3.009	2.995	3.020	3.028	3.001	3.003	3.001	2.997
Mn/(Mn+Fe)	0.27	0.29	0.30	0.33	0.30	0.31	0.79	0.84	0.84	0.81	1.00	1.00	0.97	1.00	0.97	0.99	0.99	1.00	0.97
Ta/(Ta+Nb)	0.37	0.35	0.29	0.29	0.28	0.24	0.34	0.27	0.30	0.28	0.28	0.27	0.30	0.31	0.38	0.34	0.34	0.59	0.60

p.p.: primitive pockets, e.p.: evolved pockets, a, b: two compositions of the same sample. * Mean result of eight determinations; ¶ mean result of eleven determinations, § mean result of thirteen determinations. Sample 1158[I] and 1158[II]: two different crystals were analyzed. Unit-cell parameters of selected samples: 2159: *a* 14.290(1), *b* 5.741(4), *c* 5.081(4) Å; 1144: *a* 14.452(4), *b* 5.719(4), *c* 5.094(3) Å; 1146: *a* 14.388(6), *b* 5.759(9), *c* 5.071(1) Å; 1147: *a* 14.403(4), *b* 5.747(1), *c* 5.086(1) Å; 1149: *a* 14.35(5), *b* 5.729(1), *c* 5.088(1) Å.

nocolumbite rich in W) and 30% (W-rich phase, see next section).

Very rare crystals of ferrocolumbite (samples 1188, 2159 and 1152) and manganocolumbite occur in the primitive pockets, whereas in the evolved cavities, both manganocolumbite and manganotantalite (rim of sample 2157) have been found.

"Wolframo-ixiolite"

A complex oxide with the formula $(Nb,Ta,Ti,W,Zr,Fe,Ti,Mn,U,Bi)_4O_8$, here referred to informally as "wolframoixiolite", seems to be a disordered columbite–tantalite-group mineral. The compositional resemblance to metastable high-temperature ixiolite may be ex-

plained by considering its structure, which converts, upon heating, to ordered columbite–tantalite (Nickel *et al.* 1963, Grice *et al.* 1976).

The "wolframo-ixiolite" found in the Fonte del Prete dike forms crystals that occur with U–Bi polycrase-(Y), uranopolycrase, polycrase-(Y) and columbite. Sample D, in small acicular needles, was found inside a columbite crystal, with both embedded in a K-feldspar matrix (Table 4). These needles have a very high W content (0.47–0.92 *apfu*), with the following order of site filling: Nb ≥ W ≈ Fe > Mn > Ti > Zr > Ta. The analytical results reported in Table 4, calculated on the basis of eight oxygen atoms for four cations hosted in a single site (because of structural disorder), show in some cases a lower-than-expected cation total, perhaps due to some trivalent iron or manganese.

An XRD analysis of sample D indicates that after heating at about 900°C for ten hours, an orthorhombic cell appears whose parameters are reported in Table 4, and which corresponds to a cell close to the columbite–tantalite group. The use of a single-crystal technique (precession or Weissenberg photographs) was avoided because the sample is not homogeneous.

The second sample (2162) is present as exsolution-induced blebs of "wolframo-ixiolite" in highly altered U- and Bi-rich polycrase-(Y). The W content here is lower (0.37–0.40 *apfu*), and the order of site occupancy (Nb > Mn > Ti > W > Ta > Fe) indicates a composition near that of disordered columbite. Even here, the dimensions of the crystals do not permit a detailed analysis using single-crystal X-ray methods.

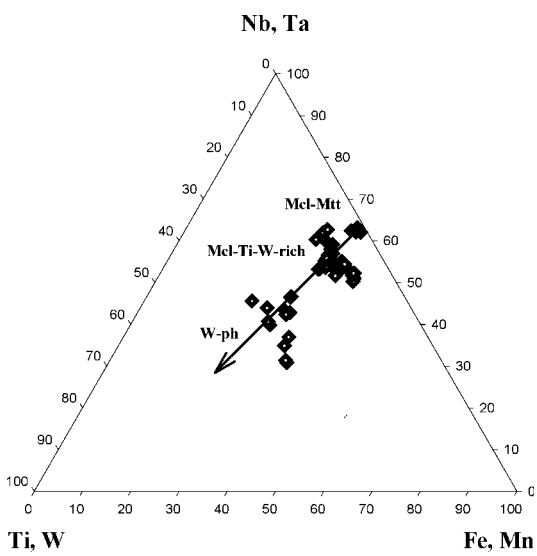

FIG. 6. Triangular plot of the occupancy of the *A* and *B* sites of the columbite–tantalite series and the W-rich phase: Ti–W-poor columbite–tantalite (Mcl–Mtt), Ti–W-rich columbite (Mcl Ti–W-rich) and "wolframo-ixiolite" (W-ph), with an arrow indicating the evolutionary trend.

Figure 6, a (Nb,Ta) – (Ti, W) – (Fe, Mn) diagram, shows the compositional area given by the phases studied, together with a trend given by the sequence: manganocolumbite and manganotantalite (Ti–W-poor), ferrocolumbite and manganocolumbite (Ti–W-rich), and "wolframo-ixiolite". The W content clearly differentiates the three compositional fields. The presence of Ti and W, even in these structures, promotes disorder (without neglecting the influence of elements such as Bi, U, Y, and Dy).

Wodginite

The wodginite group of minerals includes isostructural phases with the general formula $A_4B_4C_8O_{32}$ in which the *A* site contains Mn, Fe^{2+}, Sn^{2+}, Li and □, the *B* site, Sn^{4+}, Ti, Fe^{3+} and Ta, and the *C* site, Ta, Nb and minor amount of Ti (Ercit *et al.* 1992b). On the basis of XRD results, the crystal structure of wodginite is a superstructure of ixiolite (Nickel *et al.* 1963). Ferguson

TABLE 4. REPRESENTATIVE COMPOSITIONS OF "WOLFRAMO-IXIOLITE", FONTE DEL PRETE DIKE, ISLAND OF ELBA, ITALY

Sample	e. p. D a	e. p. D b	e. p. D c	e. p. D d	e. p. 2162 a	e. p. 2162 b
Na_2O wt%	0.00	0.00	0.11	0.00	0.00	0.00
MgO	0.00	0.00	0.29	0.38	0.12	0.25
CaO	0.00	0.26	0.00	0.46	0.33	0.29
FeO	9.75	9.25	10.99	11.32	3.21	3.09
MnO	7.12	6.60	6.09	6.35	11.02	11.28
UO_2	5.22	4.19	0.86	0.00	4.23	3.80
ThO_2	0.00	0.00	0.00	0.00	0.41	0.73
SnO_2	0.00	0.00	0.64	0.76	1.32	1.02
ZrO_2	4.99	5.89	5.10	5.13	0.88	0.73
Bi_2O_3	0.00	0.00	0.00	0.00	4.98	3.96
Y_2O_3	0.00	0.00	0.00	0.00	3.06	2.90
Nb_2O_5	26.93	34.00	29.26	22.88	30.01	34.01
Ta_2O_5	8.12	10.07	8.21	9.03	13.76	12.90
TiO_2	6.44	6.96	5.21	3.46	8.01	6.99
WO_3	30.13	21.53	31.21	40.53	17.33	16.35
Al_2O_3	0.00	0.00	0.27	0.57	0.39	0.09
Total	98.70	98.75	98.24	100.87	99.07	98.37
Structural formula based on eight atoms of oxygen						
Na *apfu*	0.000	0.000	0.019	0.000	0.000	0.000
Mg	0.000	0.000	0.037	0.050	0.016	0.033
Ca	0.000	0.024	0.000	0.043	0.031	0.027
Fe^{2+}	0.721	0.660	0.799	0.830	0.238	0.228
Mn	0.533	0.477	0.449	0.472	0.826	0.842
U	0.103	0.080	0.017	0.000	0.083	0.074
Th	0.000	0.000	0.000	0.000	0.008	0.015
Sn	0.000	0.000	0.022	0.027	0.047	0.036
Zr	0.215	0.245	0.216	0.219	0.038	0.031
Bi	0.000	0.000	0.000	0.000	0.114	0.090
Y	0.000	0.000	0.000	0.000	0.144	0.136
Nb	1.077	1.312	1.150	0.907	1.201	1.355
Ta	0.195	0.234	0.194	0.215	0.331	0.309
Ti	0.428	0.447	0.341	0.228	0.533	0.463
W	0.691	0.476	0.703	0.921	0.397	0.373
Al	0.000	0.000	0.028	0.059	0.041	0.009
Σ cations	3.964	3.956	3.975	3.971	4.048	4.021

Unit-cell parameters of sample D: *a* 14.295(7), *b* 5.733(2), *c* 5.072(2) Å. Lower-case letters: different compositions of the same sample; e.p.: evolved pockets.

et al. (1976) showed that wodginite has three cation sites, all in octahedral coordination.

The species found in the Fonte del Prete dike is titanowodginite, with Ti occupancy of the *B* site exceeding 50%. This phase occurs in cavities at the terminations of the dike, with accessory minerals such as manganoan elbaite, microlite, petalite, and pollucite, all highly evolved minerals. The titanowodginite crystals attain a few mm across, are dark brown, anisotropic, and biaxial (+).

Compositions and chemical formulae are reported in Table 5 on the basis of 32 oxygen atoms. The calculation of the formula is problematic, because several elements may be hosted in more than one site. Sample Z7, which is the most representative (Table 5), shows a composition noteworthy for its high Ti content, which is greater than what has been reported in the literature (Ercit *et al.* 1984, 1992a, b). Titanium substitutes for Ta and Sn at the *B* site, and partially for Ta and Nb at the *C* site. The unit-cell parameters are *a* 9.47(1), *b* 11.44(2), *c* 5.092(2) Å, β 91.03(6)°. The titanowodginite from the Fonte del Prete dike differs from that reported in the literature (Ercit *et al.* 1992 c) in its high Ti and Ta, lower Nb and total lack of iron.

TABLE 5. REPRESENTATIVE COMPOSITIONS OF WODGINITE, FONTE DEL PRETE DIKE, ISLAND OF ELBA, ITALY

Sample	e. p. Z7 rim	e. p. Z7 interior	e. p. Z7 core		e. p. Z7 rim	e. p. Z7 interior	e. p. Z7 core
MnO wt%	10.94	10.95	11.29	Mn *apfu*	3.679	3.720	3.831
SnO_2	5.12	6.93	8.23	Y	0.135	0.092	0.196
Y_2O_3	0.64	0.43	0.92	Ti(*A*)	0.074	0.000	0.000
Nb_2O_5	4.08	5.96	6.89	*A* site	3.888	3.812	4.027
Ta_2O_5	66.74	64.09	61.40	Sn	0.811	1.108	1.315
TiO_2	11.13	9.07	8.70	Ti(*B*)	3.189	2.736	2.685
WO_3	0.00	0.43	0.50	*B* site	4.000	3.844	4.000
				Mn	0.000	0.000	0.010
Total	98.65	98.51	97.93	Nb	0.732	1.081	1.248
				Ta	7.207	6.874	6.690
				Ti(*C*)	0.061	0.000	0.010
				W	0.000	0.045	0.052
				C site	8.000	8.000	8.000

The structural formulae are based on 32 atoms of oxygen. The unit-cell parameters of sample Z7: *a* 9.47(1), *b* 11.44(2), *c* 5.092(2) Å, β 91.03((6)°.

Microlite

Microlite occurs as a primary phase in the evolved cavities of the terminations of the Fonte del Prete dike, in association with manganocolumbite, "wolframoixiolite", titanowodginite and, rarely, manganotantalite. Minerals of the microlite subgroup of the pyrochlore group have the general formula $A_{2-m}B_2X_{6-w}Y_{1-n}{\bullet}pH_2O$, where the *A* site may be occupied by Na, Ca, *REE*, U, Th, Bi, Mn, and Fe, the *B* site, by Ta, Nb, Ti, and W, the *X* site is normally fully occupied by O, and the *Y* site, by O, OH and F; *m* has a value from 0 to 2, whereas *n* ranges from 0 to 1. On the basis of the classification of the pyrochlore group (Hogarth 1977), the Fonte del Prete dike shows only microlite (Fig. 7).

In Table 6, some compositions have sums ranging from 94.50 to 99.32 wt%; the low totals may be accounted for by the presence of H_2O. The composition of microlite from the Fonte del Prete dike is highly variable, ranging from Na-, Ca-rich to U-rich. The major elements in the *A* and *B* sites are Na (0.80–1.15 *apfu*), Ca (0.40–1.15 *apfu*), U (0–0.45 *apfu*), Ta (1.20–1.75 *apfu*), and Nb (0.24–0.77 *apfu*). A small amount of Ti and W also are present. Considering the occupancy of the *A*, *X* and *Y* sites, the Elban microlite shows a low proportion of vacancies and may be regarded as unaltered. Only a few samples (C5 and C8) show some signs of primary alteration along their rim (Lumpkin & Ewing 1988, 1992, Lumpkin *et al.* 1986). The limited degree of alteration of these samples and the limited leaching of alkalis could well be related to the young age of the pegmatite (Aurisicchio *et al.* 2001).

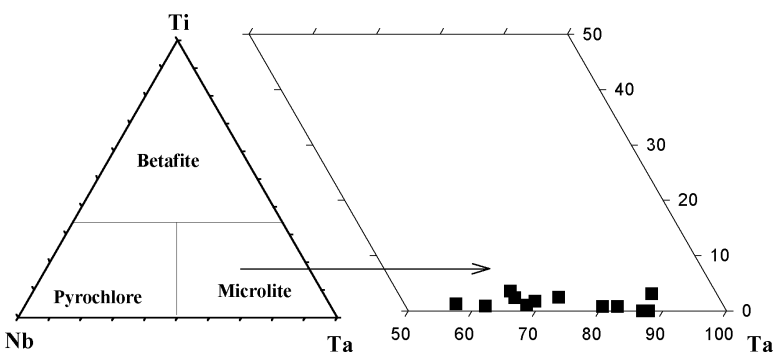

FIG. 7. Occupancy of the *B* site of the pyrochlore-group minerals according to the major elements (Hogarth 1977), showing the compositions of the microlite encountered.

Ca has a random distribution (Fig. 8a), with a minimum in the core where U is higher, whereas the U content defines an oscillatory zoning from the core to the rim of the crystal ($2Ca^{2+} \leftrightarrow U^{4+}$) (Fig. 8b). Samples C5, C8, and M2 have been heated at 900°C for 10 hours. XRD data, reported in Table 6, show a decrease in the *a* parameter as U content increases and Ca content decreases.

Discussion

The samples studied here come from primitive pockets located in the central part (core zone) of the Fonte del Prete dike and evolved pockets located at its extremities. A comparison of the Nb–Ta oxides in those pockets indicates the attainment of the highest level of fractionation (on the basis of Nb/Ta values) in the evolved pockets. A few samples belong to the intermediate zone of the massive pegmatite. On the basis of the evolutionary trend established in each Nb–Ta mineral group, we suggest a possible mechanism of evolution of the dike.

A set of Ti–Nb–Ta diagrams (Figs. 9a, b) shows the *B*-site occupancy of all phases belonging to primitive (a) and evolved cavities (b). Niobian rutile and euxenite-(Y), with high values of Ti and Nb at the *B* site, and Fe and Y + *REE* at the *A* site, occur in the intermediate zone of the massive pegmatite and in the primitive pockets. Even if the composition of euxenite-(Y) from cavities is richer in Ta, levels never reach the composition of tanteuxenite. With decreasing Nb and increasing Ti content, euxenite-(Y) gradually gives way to polycrase-

TABLE 6. REPRESENTATIVE COMPOSITIONS OF MICROLITE FROM THE FONTE DEL PRETE DIKE, ISLAND OF ELBA, ITALY

Sample	e. p. A1 rim	e. p. A1 core	e. p. C5 rim	e. p. C5 core	e. p. M2 rim	e. p. M2 core	e. p. R14 rim	e. p. R14 core	e. p. C8 rim	e. p. C8 core	e. p. 1056 mean*	e. p. 1057 mean¶
Na_2O wt %	4.75	3.83	5.85	5.60	6.34	5.95	5.86	5.82	4.69	5.28	4.79	5.34
CaO	11.85	8.16	6.52	9.23	9.36	9.06	10.15	6.05	3.98	4.24	4.89	4.78
FeO	0.00	0.00	0.00	0.00	0.23	0.00	0.00	0.00	0.00	0.00	1.17	0.00
MnO	0.00	0.00	0.00	0.00	0.00	0.00	0.00	0.20	0.04	0.47	0.64	0.69
UO_2	0.87	12.07	12.17	0.43	3.96	2.87	0.00	14.69	17.33	18.57	17.10	18.81
ThO_2	0.00	0.00	0.00	0.00	0.00	0.00	0.00	0.56	0.29	0.00	0.00	0.00
SnO_2	0.93	1.71	0.42	0.41	0.00	0.00	1.00	0.00	0.00	0.52	0.83	0.61
Y_2O_3	0.00	0.00	1.00	0.92	1.23	0.40	0.00	0.00	0.51	0.38	0.00	0.50
Nb_2O_5	6.03	4.33	18.06	10.02	15.94	8.20	6.78	19.47	12.16	10.85	13.60	14.95
Ta_2O_5	71.77	63.71	49.41	69.79	61.28	70.40	73.92	46.15	53.10	54.58	53.45	49.60
TiO_2	0.00	0.80	0.26	0.25	0.33	0.24	0.00	0.36	0.62	0.64	0.50	1.00
WO_3	1.51	2.61	2.64	0.72	0.00	0.00	0.69	0.94	1.72	1.65	1.34	0.98
ZrO_2	0.00	0.00	0.00	0.00	0.00	0.00	0.00	0.00	0.51	0.00	0.00	0.00
Al_2O_3	0.00	0.00	0.47	0.40	0.00	0.00	0.00	0.00	0.00	0.00	0.42	0.27
Total	97.71	97.20	96.80	97.77	98.67	97.12	98.54	94.50	99.32	97.79	98.73	97.53
Structural formulae based on 2.00 *B*-site cations												
Na *apfu*	0.813	0.722	0.985	0.892	1.019	1.001	0.973	1.032	0.861	0.992	0.848	0.960
Ca	1.122	0.850	0.607	0.812	0.832	0.843	0.932	0.593	0.404	0.440	0.478	0.475
Fe^{2+}	0.000	0.000	0.000	0.000	0.016	0.000	0.000	0.000	0.000	0.000	0.089	0.000
Mn	0.000	0.000	0.000	0.000	0.000	0.000	0.000	0.015	0.003	0.038	0.049	0.054
U	0.017	0.261	0.235	0.008	0.073	0.055	0.000	0.299	0.366	0.400	0.347	0.388
Th	0.000	0.000	0.000	0.000	0.000	0.000	0.000	0.012	0.006	0.000	0.000	0.000
Y	0.000	0.000	0.046	0.040	0.054	0.018	0.000	0.000	0.026	0.019	0.000	0.025
A site	1.985	1.900	1.887	1.765	1.995	1.918	1.943	1.960	1.819	1.931	1.843	1.924
Nb	0.241	0.191	0.709	0.372	0.598	0.322	0.263	0.805	0.521	0.475	0.561	0.627
Ta	1.724	1.685	1.167	1.559	1.382	1.662	1.722	1.148	1.369	1.437	1.327	1.251
Ti	0.000	0.058	0.017	0.015	0.021	0.016	0.000	0.025	0.044	0.047	0.034	0.070
W	0.035	0.066	0.059	0.015	0.000	0.000	0.015	0.022	0.042	0.041	0.032	0.024
Zr	0.000	0.000	0.000	0.000	0.000	0.000	0.000	0.000	0.024	0.000	0.000	0.000
Al	0.000	0.000	0.048	0.039	0.000	0.000	0.000	0.000	0.000	0.000	0.045	0.030
O	6.645	6.870	6.641	6.322	6.575	6.474	6.501	6.758	6.837	6.873	6.750	6.815

e.p.: evolved pockets. * mean result of seven determinations; ¶ mean result of five determinations.
Fluorine was sought and not found. Unit-cell parameter *a* of selected samples: C5: 10.416(4) Å, M2: 10.427(1) Å, 1056: 10.402(2) Å.

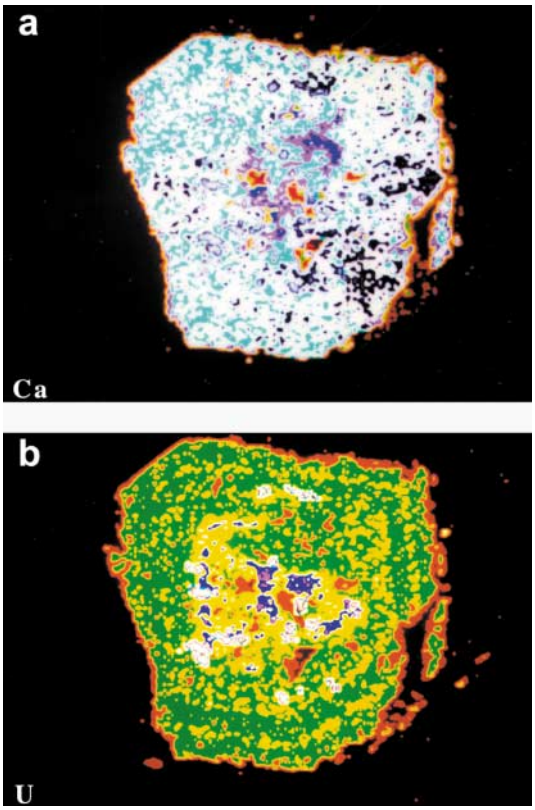

FIG. 8. X-ray maps of Ca (a) and U (b) in microlite sample A1; magnification 80×, white > light blue > pink > blue > yellow > green > red.

(Y) (Table 2, sample H14), which becomes the dominant phase, with a core rich in Y and a rim enriched in U + Bi. The *B* site of polycrase-(Y) is characterized by a sharp increase in level of Ta, which varies from about 0 to 20%, confirming the usual pattern of Nb/Ta fractionation in LCT pegmatites. In the evolved cavities, polycrase-(Y), invariably richer in U, gives way to uranopolycrase (Aurisicchio *et al.* 1993) (Fig. 5b). The Bi content of the polycrase-(Y) deserves a separate comment. This element seems prefer polycrase-(Y) instead of euxenite-(Y), giving a trend parallel to that of U. In general, Bi increases from a Bi-poor core to a Bi-rich rim, even if in some cases a cluster distribution is present (sample 2161). However, the occurrence of other Bi minerals like the sulfosalts cannizzarite and lillianite in the Elban miarolitic pegmatite (Orlandi & Pezzotta 1997) confirms the presence of Bi and can be viewed in two ways. On one hand, it indicates the transition from pegmatite to a hydrothermal stage, and on the other, it confirms the presence of Bi in the volatile-enriched residual melt.

The members of the columbite–tantalite group plot in the lower part of Figure 9a. In the primitive pockets, ferrocolumbite crystallizes, rich in Ti (~4 wt% TiO_2) and W (~6 wt% WO_3), whereas manganocolumbite and manganotantalite are found only in the pockets at the extremities of the dike (Fig. 9b). Columbite–tantalite-group minerals may be considered an excellent petrochemical indicator because of the marked fractionation in terms of Nb/Ta and Fe/Mn, which records changes in the composition of the volatile-rich residual melt, forming characteristic phases. However, one should consider also the competition between columbite–tantalite and the coexisting phases containing Nb, Ta, Fe and Mn.

In Figure 10, we report the trend Ta/(Ta + Nb) *versus* Mn/(Mn + Fe), which emphasizes the contrast in chemical compositions of the phases in the two types of cavity. In particular, ferrocolumbite, present only in the primitive pockets, shows a limited enrichment in Ta. Manganocolumbite, the manganese-dominant phase present in the pockets at the terminations of the dike, evolves directly to manganotantalite, as shown by the rim on sample 2157 (Table 3). Figure 10 reveals also two compositional gaps, the first one between the two types of pockets, linked to the degree of evolution of the host units in which the pockets grew. The second one, between rim and core of the same grain 2157, is likely linked to changes in thermal conditions.

Considering samples containing very low levels of Ti, Mulja *et al.* (1996) and Černý *et al.* (1986) ascribed the degree of order of the columbite–tantalite minerals to environmental factors (*e.g.*, rapid rate of cooling). Ercit *et al.* (1995), however, suggested that the disorder in the columbite group could promote higher levels of Ti, W, Sc and Sn. Unlike what was reported before, the Elban samples, rich in Ti and W (both >0.1 *apfu*), seem to be increasingly disordered, according to the amounts of these two cations. Samples from Fonte del Prete are all disordered; after heating, some of them become fully ordered (1144, 1145, 1146), and another (2159), partially so.

In the evolved cavities, Ta-dominant phases (microlite and wodginite) also are present, as are other W-rich species, as is typical of the LCT pegmatite family. Microlite is the Ta-dominant phase that is widespread in the evolved pockets. Together with titanowodginite and manganotantalite, the presence of microlite indicates the maximum level of fractionation reached by the volatile-rich melt. The crystals of titanowodginite found in these pockets imply that the activity of Ti, still high in the residual melt, may give rise to discrete phases.

Pegmatite evolution

The Fonte del Prete pegmatite can be classified as belonging to rare-element class, complex type of granitic pegmatite (Černý 1990). At present, it is not possible to define to what subtype it belongs. The pres-

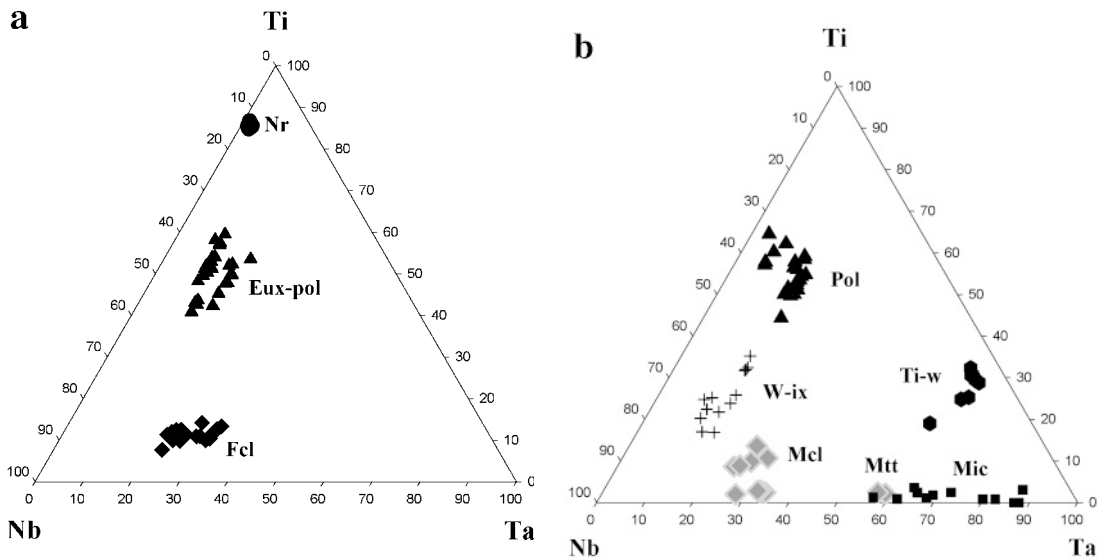

Fig. 9. Triangular Ti–Nb–Ta plot representing the distribution of the coexisting phases in the primitive and evolved pockets. a. Primitive pockets: ●: Nr (niobian rutile), ▲: Eux–pol [euxenite-(Y) – polycrase-(Y) group], ◆: Fcl (ferrocolumbite). b. Evolved pockets: ▲: Pol [U–Bi-rich polycrase-(Y) and uranopolycrase], +: W-ix ("wolframo-ixiolite"), ◆: Mcl and Mtt (manganocolumbite and manganotantalite), ■: = Mic (microlite), ⬢: Ti-w (titanowodginite).

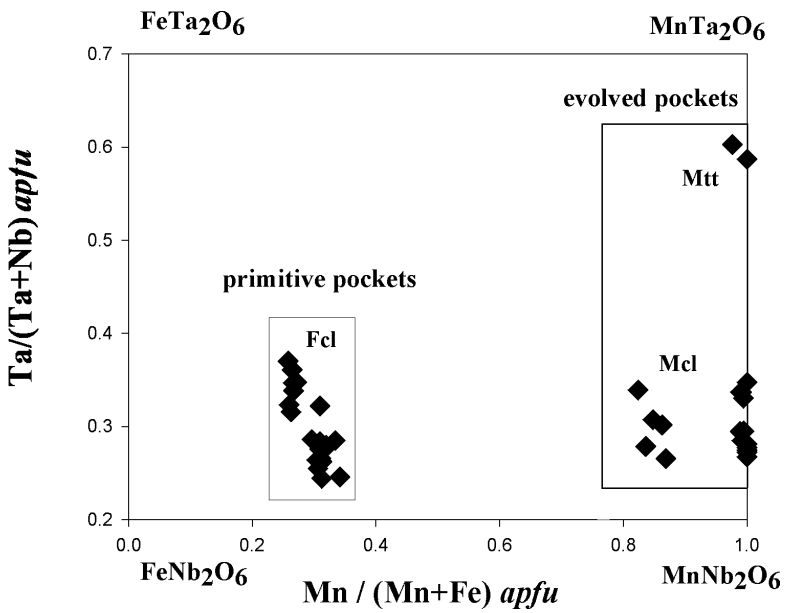

FIG. 10. Distribution of Elban columbite–tantalite minerals with the variation of the Ta/(Ta + Nb) and Mn/(Mn + Fe) values: (Fcl) ferrocolumbite; (Mcl) manganocolumbite and (Mtt) manganotantalite.

ence of some elements (Ti, Y + the heavy *REE*) typical of the rare-element type of granitic pegmatite should not be a surprise because the parent granite derives from the mixing of a peraluminous magma with batches of mantle-derived basic magma (Poli *et al.* 1989).

The dike is characterized by asymmetrical complex zoning and miarolitic pockets, as shown by its mineralogical assemblage of beryl, tourmaline, lepidolite, spessartine, and Nb–Ta oxides. A strong enrichment in boron during the entire evolution marks the LCT pegmatite at Fonte del Prete, as confirmed by the crystallization of tourmaline throughout, from the border to the core zone and in the pockets. The presence of polychrome tourmaline, ranging from schorl to elbaite, testifies to the changing compositions of the pegmatite-forming melt – fluid system with progressive crystallization, the stability of each composition being related to specific conditions of P, T, and *X* (Jolliff *et al.* 1986). In addition, the increasing Ta/(Ta + Nb) and Mn/(Mn + Fe) values observed in the columbite–tantalite group correlate positively with the degree of evolution of the dike. This pattern could be ascribed to the greater solubility of Mn and Ta in the melt and, at same time, to the presence of F, which complexes with Mn and Ta (Černý *et al*. 1985, 1986).

Two distinct stages of late crystallization have been recognized, and the differences in their degree of evolution have been documented by a detailed investigation of the mineral assemblages in terms of crystal chemistry. The early saturation of the volatile-enriched melt in a vapor phase gave rise to pockets enriched in relatively primitive phases containing Ti-, Nb-, Fe-, Y and the heavy rare-earth elements, whereas a later stage of vapor saturation gave rise to pockets containing an assemblage of evolved minerals of Mn, Ta and W.

Acknowledgements

This work was financially supported by the Italian National Council of Research scientific projects of the Centro di Studio per gli Equilibri Sperimentali in Minerali e Rocce (now IGG, CNR, Rome, Italy).

The presentation was considerably improved by critical reviews of T.S. Ercit. The authors are also indebted to editor, R.F. Martin, for a critical review, useful suggestions and extensive improvement of the English.

References

Åmli, R. & Griffin W.L. (1975): Microprobe analysis of REE minerals using empirical correction factors. *Am. Mineral.* **60**, 599-606.

Appleman, D.E. & Evans, H.T., Jr. (1973): Job 9214: indexing and least-squares refinement of other diffraction data. *U.S. Geol. Surv., Comput. Contrib.* **29** (*NTIS Doc.* **PB2-16188**).

Aurisicchio, C., Conte, A.M. & Černý, P. (1994): Petrochemical features of igneous rocks in the rare-element pegmatite field of Elba, Italy. *Int. Mineral. Assoc., 16th Gen. Meeting* (*Pisa*), *Program Abstr.*, 21OS.

_____, De Vito, C., Ferrini, V. & Orlandi, P. (1998a): Geochemistry and crystal-chemistry of Nb–Ta oxides from "Fonte del Prete" dike (Elba Island, Italy). *Int. Mineral. Assoc., 17th Gen. Meeting* (*Toronto*), *Program Abstr.*, A146.

_____, _____, _____ & _____ (1998b): Complex Ti, Nb, Ta, oxides from Baveno, Elba Island and Val Vigezzo (north of Italy). *Int. Mineral. Assoc., 17th Gen. Meeting* (*Toronto*), *Program Abstr.*, A149.

_____, _____, _____ & _____ (2001): Nb–Ta oxide minerals from miarolitic pegmatites of the Baveno pink granite, NW Italy. *Mineral. Mag.* **65**, 509-522.

_____, Orlandi, P., Pasero, M. & Perchiazzi, N. (1993): Uranopolycrase, the uranium-dominant analogue of polycrase-(Y), a new mineral from Elba Island, Italy, and its crystal structure. *Eur. J. Mineral.* **5**, 1161-1165.

Boccaletti, M. & Papini, P. (1989): Ricerche meso e microstrutturali sui corpi ignee neogenici della Toscana: l'intrusione del M. Capanne (Isola d'Elba). *Boll. Soc. Geol. It.* **108**, 699-710.

Černý, P. (1982): Anatomy and classification of granitic pegmatites. *In* Granitic Pegmatites in Science and Industry (P. Černý, eds.). *Mineral. Assoc. Can., Short-Course Handbook* **8**, 1-32.

_____ (1990): Distribution, affiliation and derivation of rare-element granitic pegmatites in the Canadian Shield. *Geol. Rundsch.* **79**, 183-226.

_____ (1991): Fertile granites of Precambrian rare-element pegmatite fields: is geochemistry controlled by tectonic setting or source lithologies? *Precamb. Res.* **51**, 429-468.

_____ & Ercit, T.S. (1989): Mineralogy of niobium and tantalum: crystal chemical relationships, paragenetic aspects and their economic implications. *In* Lanthanides, Tantalum and Niobium (P. Möller, P. Černý & R. Saupé, eds.). Springer-Verlag, Berlin, Germany (27-79).

_____, Goad, B.E., Hawthorne, F.C. & Chapman, R. (1986): Fractionation trends of the Nb- and Ta-bearing oxide minerals in the Greer Lake pegmatitic granite and its pegmatite aureole, southeastern Manitoba. *Am. Mineral.* **71**, 501-517.

_____, Meintzer, R.E. & Anderson, A.J. (1985): Extreme fractionation in rare-element granitic pegmatites: selected examples of data and mechanism. *Can. Mineral.* **23**, 381-421.

_____, Paul, B.J., Hawthorne, F.C. & Chapman, R. (1981): A niobian rutile – disordered columbite intergrowth from the Huron Claim pegmatite, southeastern Manitoba. *Can. Mineral.* **19**, 541-548.

De Vito, C (1998): *Minerali di Nb e Ta nelle pegmatiti dell'Isola d'Elba, di Baveno e della Val d'Ossola:*

caratterizzazione geochimica e cristallochimica. Degree thesis, Univ. Rome "La Sapienza", Rome, Italy.

DRAKE, M.J. & WEILL, D.F. (1972): New rare earth element standards for electron microprobe analysis. *Chem. Geol.* **10**, 1179-181.

ERCIT, T.S. (1994): The geochemistry and crystal chemistry of columbite-group minerals from granitic pegmatites, southwestern Grenville province, Canadian Shield. *Can. Mineral.* **32**, 421-438.

_____, ČERNÝ, P. & HAWTHORNE, F.C. (1984): Wodginite crystal-chemistry. *Geol. Soc. Am., Abstr. Programs* **16**, 502.

_____, _____ & _____ (1992a): The wodginite group. III. Classification and new species. *Can. Mineral.* **30**, 633-638.

_____, HAWTHORNE, F.C. & ČERNÝ, P. (1992b): The wodginite group. I. Structural crystallography. *Can. Mineral.* **30**, 597-611.

_____, WISE, M.A. & ČERNÝ, P. (1995): Compositional and structural systematics of the columbite group. *Am. Mineral.* **80**, 613-619.

EWING, R.C. (1976): A numerical approach toward the classification of complex, orthorhombic, rare earth, AB_2O_6 type Nb–Ta–Ti oxides. *Can. Mineral.* **14**, 111-119.

_____ & EHLMANN, A.J. (1975): Annealing study of metamict, orthorhombic, rare-earth, AB_2O_6 type Nb–Ta–Ti oxides. *Can. Mineral.* **13**, 942-944.

_____, SNETSINGER, K.G. & BUNCH, T.E. (1977): Euxenite from Ampangabé, Madagascar. *Can. Mineral.* **15**, 92-96.

FERRARA, G. & TONARINI, S. (1985): Radiometric geochronology in Tuscany: results and problems. *Rend. Soc. It. Mineral. Petrol.* **40**, 111-124.

FERGUSON, R.B., HAWTHORNE, F.C. & GRICE, J.D. (1976): The crystal structures of tantalite, ixiolite and wodginite from Bernic Lake, Manitoba. II. Wodginite. *Can. Mineral.* **14**, 550-560.

GARVEY, R. (1986): LSUCRIPC: least squares unit-cell refinement with indexing on the personal computer. *Powder Diffraction* **1,** 144.

GRICE, J.D., ČERNÝ, P. & FERGUSON, R.B. (1972): The Tanco pegmatite at Bernic Lake, Manitoba. II. Wodginite, tantalite, pseudo-ixiolite and related minerals. *Can. Mineral.* **11**, 609-642.

_____, FERGUSON, R.B., & HAWTHORNE, F.C. (1976): The crystal structures of tantalite, ixiolite and wodginite from Bernic Lake, Manitoba. I. Tantalite and ixiolite. *Can. Mineral.* **14,** 540-549.

HOGARTH, D.D. (1977): Classification and nomenclature of the pyrochlore group. *Am. Mineral.* **62**, 403-410.

KELLER, V.A. & PIALLI, G. (1990): Tectonics of the Island of Elba: a rappraisal. *Boll. Soc. Geol. It.* **109**, 413-425.

JOLLIFF, B.L., PAPIKE, J.J. & SHEARER, C.K. (1986): Tourmaline as a recorder of pegmatite evolution: Bob Ingersoll pegmatite, Black Hills, south Dakota. *Am. Mineral.* **71**, 472-500.

LUMPKIN, G.R., CHAKOUMAKOS, B.C. & EWING, R.C. (1986): Mineralogy and radiation effects of microlite from the Harding pegmatite, Taos County, New Mexico. *Am. Mineral.* **71**, 569-588.

_____, & EWING, R.C. (1988): Alpha-decay damage in minerals of the pyrochlore group. *Phys. Chem. Minerals* **16**, 2-20.

_____ & _____ (1992): Geochemical alteration of pyrochlore group minerals: microlite subgroup. *Am. Mineral.* **77**, 179-188.

MULJA, T., WILLIAMS-JONES, A.E., MARTIN, R.F. & WOOD, S.A. (1996): Compositional variation and structural state of columbite–tantalite in rare-element granitic pegmatites of the Preissac–Lacorne batholith, Quebec, Canada. *Am. Mineral.* **81**, 146-157.

NICKEL, E.H., ROWLAND, J.F. & MCADAM, R.C. (1963): Wodginite – a new tin–manganese tantalite from Wodgina, Australia, and Bernic Lake, Manitoba. *Can. Mineral.* **7**, 390-402.

ORLANDI, P. & PEZZOTTA F. (1997): *Minerali dell'Isola d'Elba*. Edizioni Novecento Grafico, Bergamo, Italy.

PEZZOTTA, F. (1993): Osservazioni strutturali, petrografiche e classificative sui filoni aplitico-pegmatitici litiniferi del settore occidentale del M.te Capanne (Isola d'Elba). *Plinius* **10**, 208-209.

_____ (2000): Internal structures, parageneses and classification of the miarolitic (Li-bearing) complex pegmatites of Elba Island (Italy). *Mem. Soc. It. Sci. Nat. e Mus. Civ. St. Nat., Milano* **30**, 29-43.

POLI, G., MANETTI, P. & TOMMASINI, S. (1989): A petrological review on Miocene–Pliocene intrusive rocks from southern Tuscany and Tyrrhenian Sea (Italy*). Per. Mineral.* **58**, 109-126.

ROEDER, P.L. (1985): Electron-microprobe analysis of minerals for rare-earth elements: use of calculated peak-overlap corrections. *Can. Mineral.* **23**, 263-271.

Received November 3, 2001, revised manuscript accepted May 7, 2002.